ACS Sustainable Chemistry & Engineering

Research Article

pubs.acs.org/journal/ascecg

Deactivation of Pt Catalysts during Hydrothermal Decarboxylation of Butyric Acid

Thomas Yeh, Suljo Linic, and Phillip E. Savage*

Chemical Engineering Department, University of Michigan, Ann Arbor, Michigan 48109-2136, United States

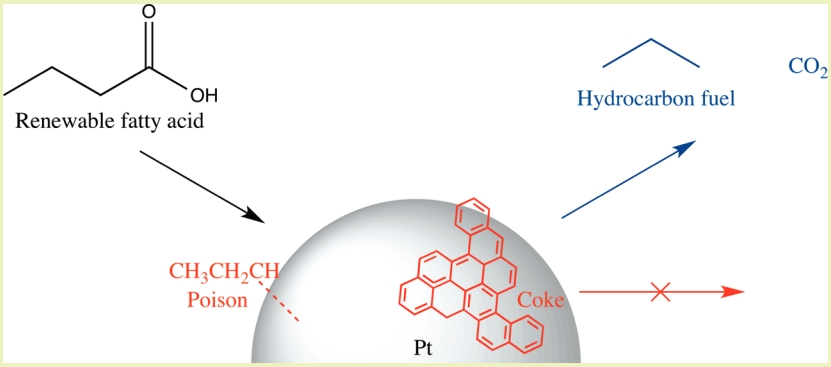

ABSTRACT: Decarboxylation of fatty acids is a path to hydrocarbon fuels from renewable biomass resources. We explored the deactivation of Pt catalysts during the hydrothermal decarboxylation of butyric acid at 350 °C and 3000 psi in a continuous flow reactor. DRIFTS spectra of the used catalyst showing characteristic absorptions at 2900 and 1500 cm^{-1} suggested that unsaturated hydrocarbons are responsible for catalyst poisoning. The restoration of appreciable catalyst activity due to controlled oxidation indicated that coke had formed during the decarboxylation experiment. BET measurements showed that the Vulcan XC-72R carbon support pore volume decreased from 1.41 to 0.55 cm^3/g. Thus, a combination of poisoning, coking, and pore structure changes in the carbon support caused the Pt/C catalyst to deactivate over a period of 24 h on stream. The first-order deactivation rate constant for Pt/C was 0.063 ± 0.006 h^{-1}. These results provide insight into interventions that may lead to prolonged catalyst activity for hydrothermal reactions.

KEYWORDS: *High temperature water, Butyric acid, Fatty acid, Platinum, Deactivation*

INTRODUCTION

In response to concerns related to energy supply, anthropogenic CO_2 emissions, and domestic energy security, research has been directed to find potential alternatives to petroleum-derived liquid fuels for transportation. Potential solutions include electricity, hydrogen, and bioderived liquid fuels. Liquid fuels, and especially hydrocarbons, have advantages over electricity and hydrogen due to compatibility with the existing transportation infrastructure, ease of storage and transportation of the fuel, and high energy density.

Many oil-producing plants such as soy, jatropha, and algae could be viable sources of renewable liquid fuels. Animal fats, grease, and waste cooking oils can similarly be converted to fuel. These oils and fats comprise triglycerides and fatty acids that can be converted to hydrocarbons, which would be compatible with the existing infrastructure for distribution and use of liquid transportation fuels. These renewable resources are of biological origin; hence, they have a high moisture content. Removing this water prior to processing requires energy for drying and reduces the overall energy efficiency of any biofuel production process. Moreover, there are several proposed biofuel production processes that involve triglyceride hydrolysis in hot compressed water and hence produce fatty acid-containing aqueous streams.[1−4] Additionally, hydrothermal liquefaction of microalgae produces an aqueous effluent stream that is rich in fatty acids.[5] These fatty acids are soluble in water at the elevated temperatures employed. Although one could separate the fatty acids in these streams from the water (e.g., by cooling the effluent and then extracting the fatty acids in an organic solvent) and then convert the fatty acids to hydrocarbons in a second processing step, there are advantages to performing this catalytic conversion directly in the aqueous phase in a single step. Doing so would provide process simplification (eliminate a separation step), reduce process energy demands (obviate cooling the effluent from the hydrolysis or liquefaction reactor and then heating the fatty acids again prior to their conversion to hydrocarbons), and facilitate product recovery (hydrocarbons are easier to separate from water by decanting than are fatty acids). Thus, there is considerable interest in the aqueous-phase conversion of fatty acids to hydrocarbons.[6−13]

Received: July 3, 2014
Revised: August 26, 2014
Published: September 2, 2014

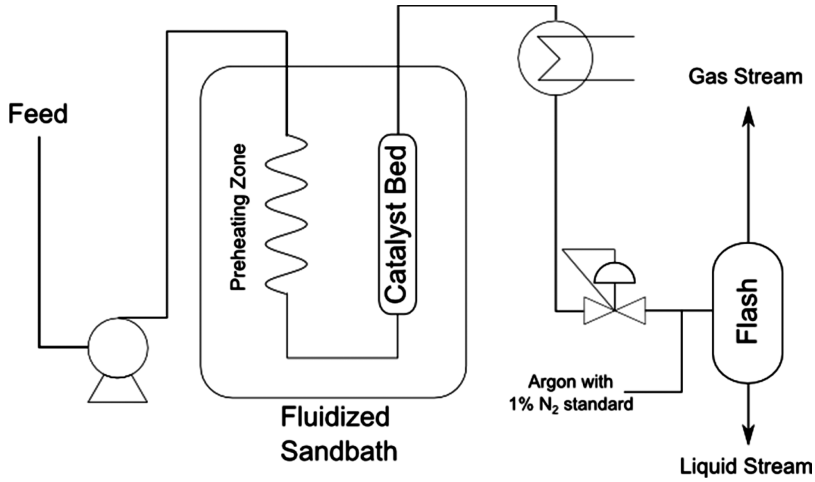

Figure 1. Hydrothermal catalytic flow reactor schematic.

The path to hydrocarbon fuel molecules from fatty acids is to remove oxygen atoms, either as water via hydrogen addition and hydrodeoxygenation (HDO) or as carbon dioxide via decarboxylation. Decarboxylation offers an advantage over HDO in that there is no stoichiometric need for added hydrogen.

Catalytic decarboxylation (and decarbonylation) of fatty acids has largely been studied in the gas phase or in condensed organic phases. Saturated fatty acids have received more attention than unsaturated ones, and the literature provides evidence of catalyst deactivation.[14,15] For example, the Pd/C catalysts used for lauric acid decarboxylation deactivated in less than 20 min due to the generation of coke and CO.[14] A separate study with stearic acid revealed that pore collapse within the support was responsible for much of the catalyst deactivation in that system.[16] Unsaturated fatty acids show catalyst deactivation to an even greater degree than observed in reactions with saturated fatty acids;[9] they typically undergo hydrogenation of the double bond to form a saturated fatty acid prior to the decarboxylation step. A study of oleic acid decarboxylation with added H_2 showed that the fatty acid went through a stearic acid intermediate prior to decarboxylation. The Pd/C catalyst also experienced deactivation from what was suspected to be coke.[17] Regeneration of decarboxylation catalysts has been attempted via reduction in hydrogen under the same reaction temperature, but in all cases, the deactivation was irreversible.[14−16]

All of the aforementioned literature involves studies in a liquid organic or gas phase. As such, this prior work does not relate directly to catalytic decarboxylation in an aqueous phase. Indeed, many catalysts that are stable and active in organic media or in the gas phase are not stable in a condensed aqueous phase. Elliott and co-workers, for example, have shown that many catalyst metals, namely, Zn, W, Mo, Zn, Cr, Re, Sn, and Pb, are susceptible to performance-degrading oxidation in hot, compressed, liquid water.[18] Additionally, many supports, such as γ-alumina, that are stable in organic- and gas-phase environments are unstable in a hydrothermal environment.[19,20]

The only prior information on catalyst activity maintenance for hydrothermal decarboxylation of fatty acids is from a few experiments done previously in our lab. Pt/C and Pd/C were used in three successive 90 min batch experiments. The Pd/C catalyst showed reduced activity after each run, whereas the Pt/C catalyst was recycled without measurable loss of activity during the 4.5 h of use.[8]

Taken collectively, the literature suggests that catalyst deactivation during hydrothermal decarboxylation of fatty acids may be a potential problem for this route to renewable transportation fuels. To our knowledge, there has been no prior work dedicated to quantifying and understanding causes of catalyst deactivation in such systems. Because Pt is an active and selective decarboxylation catalyst for saturated fatty acids in both organic and hydrothermal environments[8,9,21,22] and because Pt/C was the more stable material in the previous batch reactor studies, we decided to use Pt/C in this present study. Additionally, because prior work examined activity in a batch system and just for 4.5 h of use, we decided to examine activity in a flow reactor system for much longer times on stream. The purpose of this work is to determine deactivation characteristics of Pt catalysts during the decarboxylation of carboxylic acids in hot compressed water. We selected naturally occurring butyric acid rather than a longer fatty acid as the reactant for experimental convenience. Butyric acid enjoys a sufficiently high solubility in water at ambient conditions that a feed solution for the flow reactor could be prepared conveniently. One can reasonably expect the catalytic decarboxylation chemistry for butyric acid to mimic that of larger fatty acids because the reaction of interest at the COOH group is not likely to be affected by additional methylene units that are far removed. We also note that butyric acid has been used previously in a detailed mechanistic study of decarboxylation,[23] which provides an opportunity to connect the experimental results in this study with those from DFT calculations in the prior work.

MATERIALS AND METHODS

All materials were used as received. Chloroplatinic acid hexahydrate with ≥37.50% Pt basis was from Sigma-Aldrich. Vulcan XC-72R carbon black with a particle size of ∼50 nm[24] was from Cabot Corp. P25 aeroxide titania with a particle size of <25 nm was from Evonik Industries. All gases (i.e., ultra high purity H_2, 1% N_2 in Ar, 1% H_2 in N_2) were from Cryogenic Gases, and butyric acid ≥99% was from Sigma-Aldrich. Deionized water was produced in-house and sparged with Ar prior to use.

Catalyst Synthesis. Supported Pt catalysts were prepared using incipient wetness impregnation. An aqueous solution of the metal precursor, $H_2PtCl_6{\cdot}6H_2O$, was added dropwise to the continuously stirred support, either carbon or titania. The catalyst was subsequently

crushed using a mortar and pestle and then reduced at 500 °C for 6 h under flowing 1% H_2 with a balance of N_2. After reduction, the catalyst was stored until ready for use.

Flow Reactor Procedure. Reactions were performed in a continuous flow reactor system assembled from stainless steel tubing and Swagelok parts. The reactor feed, an aqueous solution of 0.2 M butyric acid, was held in a vessel pressurized with Ar to 100 kPa. The feed stream passed through a 0.2 μm filter and was pumped into the reactor system using a ChromTech Series III HPLC pump. The preheating zone was a 1.8 m section of 1/16 in. diameter thick-walled tubing. It was connected to the catalyst bed (150 mg), consisting of a 1/4 in. diameter tube and metal frits to contain the catalyst by two reducing unions. The preheater and reactor resided in a Techne SBL-2D fluidized sand bath with a Techne TC-8D temperature controller and a type K thermocouple. The reactor effluent traveled through a 1.5 m long 1/8 in. diameter tube to a water-cooled heat exchanger. The pressure of the cooled effluent then was reduced from 21 MPa to ambient pressure using a Tescom back-pressure regulator. After the pressure let-down, Ar with 1% N_2 flowing at 5 mL/min at STP (21.1 C and 1 atm) was added to the product stream using a mass flow controller. Figure 1 shows a schematic of the key components of the flow reactor system.

Prior to each run, we leak tested the entire reactor system to at least 28 MPa at room temperature. The reactor was then placed into the sand bath at 250 °C, and hydrogen flowed through the reactor system for 1 h to reduce the catalyst. After reduction, we set the back-pressure regulator to 21 MPa and the sand bath temperature to 350 °C. We initiated flow of the 0.2 M butyric acid solution when the sand bath reached 340 °C. The ratio of the volumetric flow rate of the reactor feed (v) to the mass (W) of the catalyst (support included) was 300 mL/mg min at ambient conditions. The reaction was run continuously at this nominal steady state for 24 h to investigate the effect of aging on the catalysts.

Product Analysis. The product gases flowed to an online Agilent 6890 gas chromatograph with a thermal conductivity detector (GC-TCD) equipped with a 80/100 Porapak Q 6 ft × 1/8 in. packed column. The Ar carrier gas flowed through the column at 44 mL/min. The oven temperature was held at 40 °C for 10 min and then was increased to 225 °C at 10 °C/min. The sample collection was automated with a Lego mindstorms robot designed in-house and controlled using an RCX 2.0 controller.

Liquid samples were taken using a Gilson 223 sample changer and analyzed on an Agilent 7890 gas chromatograph with a flame ionization detector (GC-FID) equipped with a 30 m × 0.32 mm × 0.25 μm DB-FFAP column. The GC inlet was set to a split ratio of 50:1 with a temperature of 220 °C. The carrier gas flow rate through the column was set to 20 mL/min. The oven temperature started at 50 °C and was increased to 100 °C at a rate of 5 °C/min. The FID was set to 300 °C with a H_2 flow rate of 40 mL/min, air flow rate of 345 mL/min, and makeup flow of N_2 at 5 mL/min.

Catalyst Characterization. At the end of the run, the sand bath heater was turned off, and no additional steps were taken to cool the reactor. Once the reactor had cooled, deionized water at room temperature was pumped through the reactor for 1 h at approximately 0.5 mL/min to clear the system of any residual reactants. The spent catalyst was then removed from the reactor and dried at 75 °C prior to further characterization.

The catalysts were characterized using a variety of methods. X-ray diffraction (XRD) was performed with a Rigaku Rotaflex or a Rigaku Miniflex 600 and subsequently analyzed using the Jade software package. The effective metal loadings were measured using inductively coupled plasma−optical emission spectroscopy (ICP-OES), and the particle size was measured using a JEOL 2010F transmission electron microscope (TEM). Diffuse reflectance infrared Fourier transform spectroscopy (DRIFTS) was performed using a Nicolet 6700 FTIR from ThermoScientific equipped with a praying mantis cell. BET and pore size measurements were performed by heating the catalyst sample at 300 °C in He for 3 h. After heating, the samples were cooled and inserted into a Micromeritics ASAP 2010 for analysis.

Batch Reactor Procedure. We conducted a few experiments with just catalyst and water in batch mini-reactors fashioned from one 3/8 in. Swagelok cap, corresponding port connector, 3/8 to 1/8 in. reducing union, and 23 cm of 1/8 in. thick-walled tubing that connected to a right angle valve from the High Pressure Equipment Company. The reactor was filled with water such that 95% of its volume would contain liquid water at the reaction conditions, and approximately 5 mg of catalyst was added in addition to this amount of water. The reactors were then sealed and placed in a preheated fluidized sand bath. After the desired time had elapsed, the reactors were removed from the sand bath and submerged into room-temperature water to quench the reaction. The reactors were charged with 100 psig of Ar upon cooling, and the gaseous products were analyzed chromatographically as described above.

RESULTS AND DISCUSSION

This presentation of results is apportioned into three main subsections. We first discuss the various reaction products observed during the hydrothermal decarboxylation of butyric acid and from these data infer the existence of different side reactions that accompany the desired decarboxylation reaction. We then present data for catalyst activity as a function of time on stream and use the data to model quantitatively the catalyst deactivation kinetics. The final section discusses different mechanisms of catalyst deactivation and experimental results that allow discrimination among several of the possibilities.

Reaction Products. We monitored the reaction products in both the gas and liquid phases that emerged from the flow reactor. The liquid phase contained only unreacted butyric acid, whereas the gas-phase products were H_2, CO_2, CH_4, C_2H_6, and C_3H_8. No ethylene or CO was observed. The most abundant products were C_3H_8 and CO_2, indicating that Pt/C is selective for the desired decarboxylation reaction shown in Figure 2.

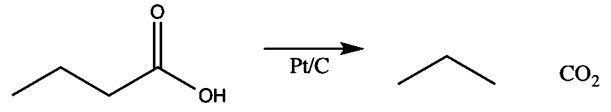

Figure 2. Butyric acid decarboxylation.

This outcome is in agreement with other work[9] on the hydrothermal conversion of saturated fatty acids over Pt/C. Over 90% of the converted butyric acid was converted to propane, and the selectivity to the decarboxylation products remained high throughout the duration of the reaction.

Figure 3 shows that the gas- and liquid-phase products together accounted for 95 ± 3% (excluding the point at t = 0.07 h) of the total carbon of the feed stream, thus effectively closing the carbon balance.

The product stream contained H_2, a product that is not formed in the decarboxylation reaction. Additionally, the H/C atomic ratio for the gas-phase products (Figure 4) modestly exceeds 2.0, the H/C ratio in butyric acid. Figure 4 also shows that the molar ratio of CO_2/C_3H_8 exceeds the stoichiometric ratio of 1.0. These results are consistent with the existence of one or more side reactions that produce modest amounts of H_2 and/or CO_2.

There are several such potential side reactions, and we consider two here. The first is steam reforming of the butyric acid reactant or the propane product. The reaction below shows the stoichiometry for the case of butyric acid, and it is clear that such a reaction could produce H:C atomic ratios well in excess of two.

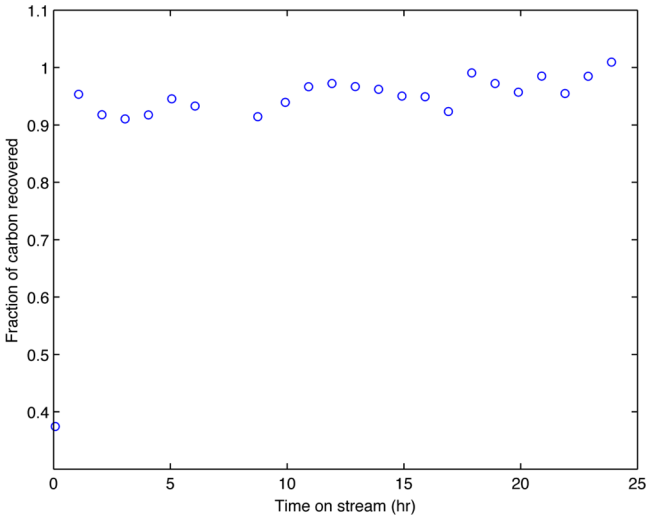

Figure 3. Carbon recovery in gas- and liquid-phase reactor effluent from hydrothermal treatment of butyric acid over Pt/C.

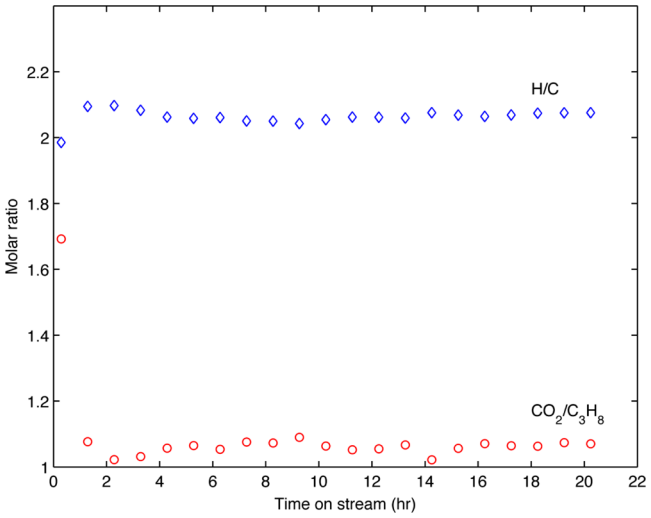

Figure 4. H/C and CO_2/C_3H_8 ratios from hydrothermal treatment of butyric acid over Pt/C.

$$CH_3CH_2CH_2COOH + 6H_2O \rightarrow 4CO_2 + 10H_2$$

We used Aspen Plus process simulation software to calculate the equilibrium compositions of butyric acid and its anticipated reaction products with water, namely, C_1, C_2, and C_3 hydrocarbons, CO_2, CO, and H_2 at the reaction conditions. We selected the thermodynamic package, SRK-KD, because of its ability to handle interactions between organic molecules and water at elevated temperatures and pressures. The RGIBBS block, which minimizes the Gibbs' free energy for the system, was chosen to calculate the equilibrium compositions for a 0.1 M aqueous stream of butyric acid at 3000 psig and 350 °C. Table 1 shows the results, which indicate that the gaseous products would have a H/C ratio of 2.6 at equilibrium and that CO_2 is formed. Both of these outcomes are consistent with the experimental observations. The equilibrium calculation gave no evidence for the presence of C_2 or C_3 hydrocarbons.

A second possible side reaction is degradation of the carbon support as shown below.

$$C + 2H_2O \rightarrow CO_2 + 2H_2$$

Table 1. Equilibrium Composition of Products from Hydrothermal Decomposition of Butyric Acid at 350 °C and 3000 psig

species	mole fraction (dry basis)
H_2	0.044
CO	<0.002
CO_2	0.360
CH_4	0.593

Carbon is generally considered a stable support in hydrothermal environments, although carbon gasification in supercritical water has been documented.[25]

The results presented thus far clearly show that the main decarboxylation reaction is accompanied by one or more minor side reactions that may involve a reactant, product, or catalyst support. The number of potentially significant side reactions is larger in this hydrothermal system due to the presence of water, which is reactive at elevated temperatures. Side reactions appear regularly in hydrothermal catalytic reaction systems and frequently complicate the interpretation of experimental results.

Minor hydrocarbon products that appeared during the nominal decarboxylation reaction include ethane and methane. These saturated alkanes are completely analogous to the *n*-alkanes Fu et al.[8,9] reported as minor products from the hydrothermal treatment of palmitic acid over Pt/C. Figure 5

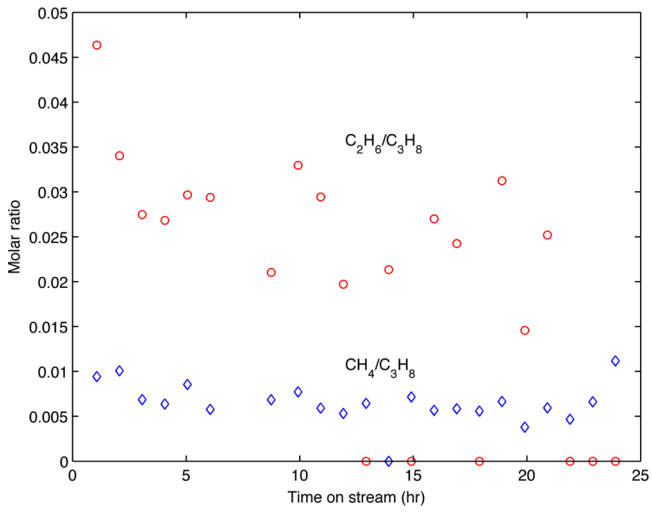

Figure 5. Molar ratios of lower alkanes to propane for hydrothermal treatment of butyric acid over Pt/C.

shows that the yields of ethane and methane were about a factor of 30−200 lower than the yield of propane. The carbon contained in these C_1 and C_2 hydrogenolysis products accounts for less than 2% of the carbon in the gas-phase reaction products with Pt/C. The scatter in experimental data is due to the concentrations of methane and ethane in the reactor effluent being near the lower detection limits of the GC-TCD.

Deactivation Kinetics. Previous work showed that fatty acid hydrothermal decarboxylation at 380 °C with Pt/C occurred in the intrinsic kinetics regime.[8] Additionally, the catalyst bed in the present experiments is essentially isothermal with a calculated temperature change of less than 1 °C. Therefore, we do not expect heat or mass transfer effects to be influencing the rates measured in the present experiments. Moreover, we do not expect the carbon support to be a major

contributor to the decarboxylation activity, as previous work showed that activated carbons were much less active than Pt/C for hydrothermal decarboxylation. Comparing activated carbon and Pt/C for stearic acid and palmitic acid show rate constants at 350 °C of 0.00075 and 0.024 1/min, respectively.[8,26] The difference in rate constants shows that catalytic effects from carbon are negligible in comparison to Pt.

The literature indicates that first-order kinetics adequately describes the hydrothermal decarboxylation of long-chain saturated fatty acids over Pt/C.[8] Combining a first-order rate equation with the design equation for the plug-flow packed-bed catalytic reactor used in the experiments and rearranging leads to the equation below, where k' is the first-order rate constant, v is the volumetric flow rate, W is the catalyst mass, and X is the conversion of butyric acid. The conversion was calculated as the ratio of the molar flow rate of carbon in the effluent gas stream divided by the molar flow rate of carbon into the reactor.

$$k' = -\frac{v}{W}\ln(1 - X)$$

Figure 6 shows the first-order rate constant as a function of time on stream for three independent runs performed under

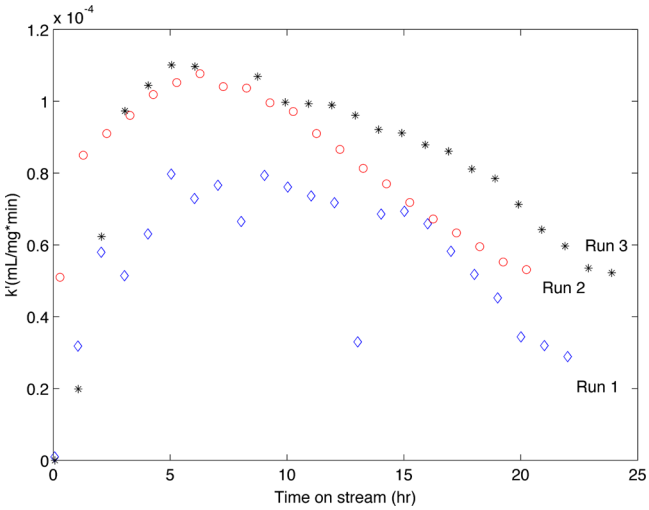

Figure 6. Variation of first-order rate constant with time on stream for hydrothermal decarboxylation of butyric acid over Pt/C at 350 °C.

nominally identical reaction conditions. The rate constant serves as a proxy for the catalyst activity. The data at times longer than 10 h provide information about the rate of catalyst activity decay. The data at shorter times on stream are not as useful. These data seem to show that the catalyst activity increases for the first 6 h on stream, and then it begins to decrease. This initial apparent increase in activity is not physical but rather an artifact due to a time lag in the flow system downstream of the reactor bed and the mixing of the initial reactor effluent with residual gas in the flash column. That is, it takes several hours after starting the experiment for the gas being analyzed by the GC to have the same composition as the gas leaving the catalyst bed. We verified this explanation by modeling the reactor as having a continuously decreasing activity and treating the flash column, which has a residence time of about 30 min under the experimental conditions, as a perfectly mixed stirred tank. This simple dynamic model clearly showed that one expects to observe an initial increase in the product concentration in the effluent with time on stream before observing a decrease with time that accurately reflects the catalyst activity loss occurring in the catalyst bed. The effect of mixing downstream of a catalytic flow reactor leading to apparent increasing catalyst activity has also been observed elsewhere.[27]

Becasue the subset of the data wherein the activity appears to increase with time does not reflect what is occurring in the catalyst bed, we exclude those portions of the data in Figure 6 from consideration when analyzing the deactivation kinetics. We consider only the data after 10 h on stream because the rate constant is decreasing within that region. We treat the rate of catalyst activity loss as being first order. With this model for the deactivation kinetics, one expects the rate constant for butyric acid conversion to decrease exponentially with time on stream, as indicated below

$$k'(t) = k'_0 e^{-k_d t}$$

where k_d is the rate constant for catalyst deactivation and k'_0 is the decarboxylation rate constant expected for a fresh catalyst. Both k_d and k'_0 were calculated by fitting $\ln(k'(t))$ to linearized data. This model captures the trends in the three independent runs in Figure 6 and gives a reasonable representation of the experimental data for the deactivation of the Pt/C catalyst. The deactivation rate constants determined from the three independent runs are 0.059, 0.062, and 0.070 h^{-1} with the respective k'_0 values of 1.58×10^{-4}, 1.84×10^{-4}, and 2.19×10^{-4} mL mg^{-1} min^{-1}. These values are all similar, which suggests that the three independent experiments provided reproducible results regarding the rate of catalyst activity decay. The best estimates (i.e., the mean value) for the deactivation rate constant and k'_0 value at 350 °C are 0.063 ± 0.006 h^{-1} and $1.9 \times 10^{-4} \pm 0.3 \times 10^{-4}$ mL mg^{-1} min^{-1}.

The results in Figure 6 provide new insights into the hydrothermal activity maintenance of Pt/C catalysts for fatty acid decarboxylation. Previous work in batch reactors[8] showed little decline in activity when Pt/C was reused in subsequent experiments, but the total time the catalysts were in use under reaction conditions was just 4.5 h. Moreover, the process used to recover the catalyst after each batch experiment and prepare it for the next may have altered the catalyst in some way and restored its activity. The present experiments, wherein the same catalyst particles were used continuously for 24 h, provide results that are more meaningful as they more closely mimic the mode of operation anticipated at a commercial scale.

Cause of Deactivation. Having demonstrated that the Pt/C catalyst loses activity with time on stream, we next consider several potential causes of the catalyst deactivation. The catalyst synthesis method was chosen, in part, to produce Pt particles larger than those in commercial catalysts to ameliorate potential sintering effects. The possibility of sintering, the combination of Pt crystallites to form larger particles with fewer exposed metal atoms, however, still needs to be investigated. XRD is one method of estimating the average size of the metal crystallites in a catalyst. Figure 7 shows the XRD spectra of the fresh Pt/C catalyst and the material recovered after 24 h on stream in the flow reactor. The crystallite size, τ, was calculated using the Scherrer equation.

$$\tau = \frac{K\lambda}{\beta \cos\theta} \quad (1)$$

We took the shape factor, K, to be 0.9. The wavelength of the X-ray radiation, λ, was 1.5406 Å. The full width at half max, β,

dx.doi.org/10.1021/sc500423b | ACS Sustainable Chem. Eng. 2014, 2, 2399−2406

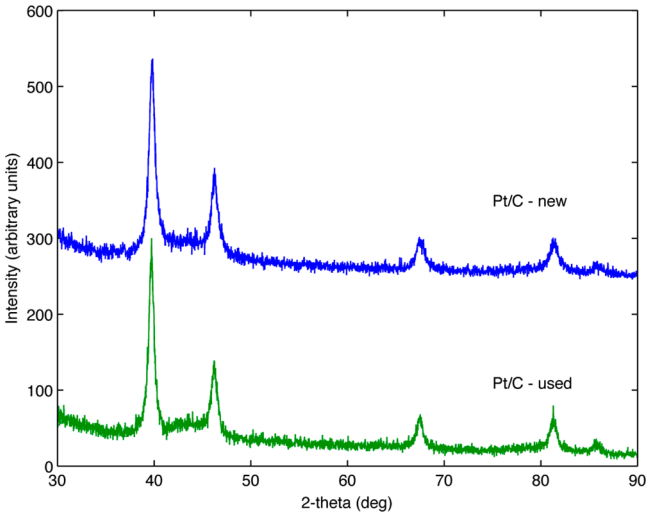

Figure 7. XRD spectra of fresh and used Pt/C catalysts.

and the Bragg angle, θ, are obtained from the XRD spectrum. From the Pt(111) XRD peaks in Figure 7, which appear at $2\theta = 40°$, the Scherrer equation showed the crystallite sizes in the fresh and used catalyst to be 13.7 and 12.3 nm, respectively. The crystallite sizes being similar in both the fresh and used catalysts suggests that loss of active area through sintering was not a major contributor to deactivation during hydrothermal decarboxylation.

TEM images in Figure 8 show that the Pt particles were 9.3 ± 3.5 nm for the fresh catalysts and 9.2 ± 3.1 nm for the used

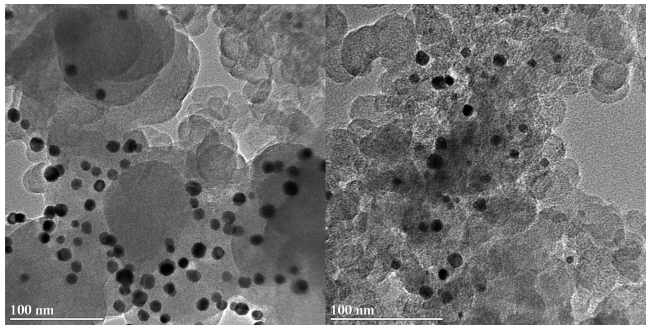

Figure 8. TEM images of fresh (left) and used (right) Pt/C catalysts.

catalyst supporting that sintering was not responsible for deactivation. This combination of XRD and TEM analyses show catalyst sintering is not a likely cause of the observed deactivation.

Another possible cause of catalyst deactivation is poisoning, which is the very strong adsorption of molecules onto the catalyst sites. Carbon-containing molecules on metal surfaces can be detected by different spectroscopic techniques. Because the catalyst support itself was carbon, however, we could not perform these traditional tests on the Pt/C catalyst. Therefore, to test the hypothesis that poison molecules might have contributed to a decrease in catalytic activity, we synthesized a catalyst containing Pt nanoparticles supported on P25 TiO_2 (80% anatase with the balance of rutile). We chose TiO_2 as an alternative support to elucidate the deactivation mechanism. TiO_2 would also allow for oxidative regeneration of the catalyst.

Figure 9 displays DRIFTS spectra of the P25 TiO_2 support, fresh Pt/TiO_2 catalyst, used Pt/TiO_2 catalyst as recovered from

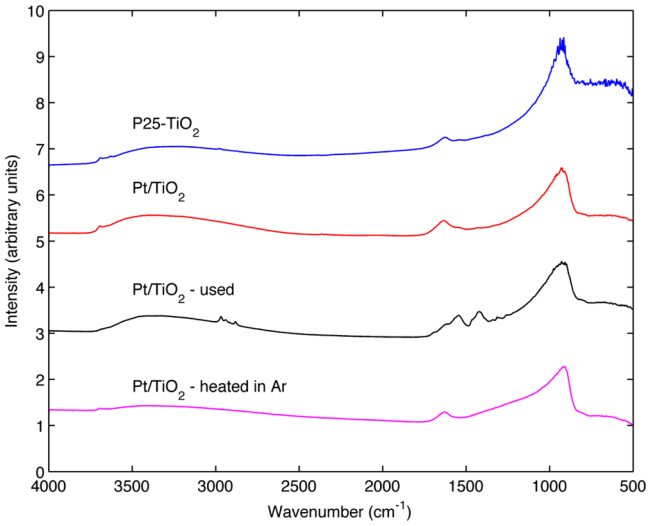

Figure 9. DRIFTS spectra for TiO_2 and Pt/TiO_2 catalysts.

the flow reactor at the end of a 24 h run, and the same material after being heated in Ar at 700 °C for 2 h. The spectra for the support and fresh catalyst are largely indistinguishable, whereas the spectrum for the used catalyst shows stretches at 2900, 1530, and 1440 cm^{-1} that were absent in the fresh material. The peak at 2900 cm^{-1} is characteristic of C−H stretches, and the peaks at 1530 and 1440 cm^{-1} are characteristic of unsaturated C−C bond stretches. The appearance of these new peaks indicates the presence of organic compounds on the catalyst surface. These organic molecules could range from being individual small molecules to being large condensed aromatic structures that adhere strongly to the surface. To assess whether the organic compounds would simply desorb, we heated the used Pt/TiO_2 catalyst to 700 °C in flowing Ar. The resulting DRIFTS spectrum is nearly identical to that of the fresh catalyst, and the peaks at 1500 and 2900 cm^{-1} present in the used catalyst are now absent. This result suggests that the organic surface species desorbed during the high-temperature treatment. Larger molecules, such as large carbon networks associated with coke formation, would not be expected to desorb in an inert environment. Typically, an oxidizing environment is needed to burn coke off a catalyst surface. These results suggest that poisoning may play a role in catalyst deactivation during hydrothermal decarboxylation of butyric acid.

Possible poisons in this system are propylene or some other C_3 hydrocarbon. Propane is the main hydrocarbon product, and Pt is known as a good dehydrogenation catalyst. To test the hypothesis that propylene or some variant thereof was a poison, we conducted an experiment wherein a Pt/C catalyst used in the flow reactor for a 24 h reaction and then reduced in place by flowing hydrogen over the catalyst at 350 °C for 1 h. We collected the gases emerging from the reactor system and analyzed them by GC. The gas contained trace amounts of propane, suggesting that unsaturated C_3 hydrocarbons had been adsorbed on the surface of the catalyst and then hydrogenated to propane during the reduction of the catalyst in flowing hydrogen. The presence of propylene on the catalyst surface would be consistent with features of the DRIFTS spectrum shown in Figure 9 for the used Pt/TiO_2 catalyst.

Following the DRIFTS experiment and the capturing of hydrogen gas with traces of propane, we investigated the

reversibility of the deactivation of a Pt/TiO_2 catalyst. Results for a 24 h run with fresh catalyst appear in Figure 10. The used

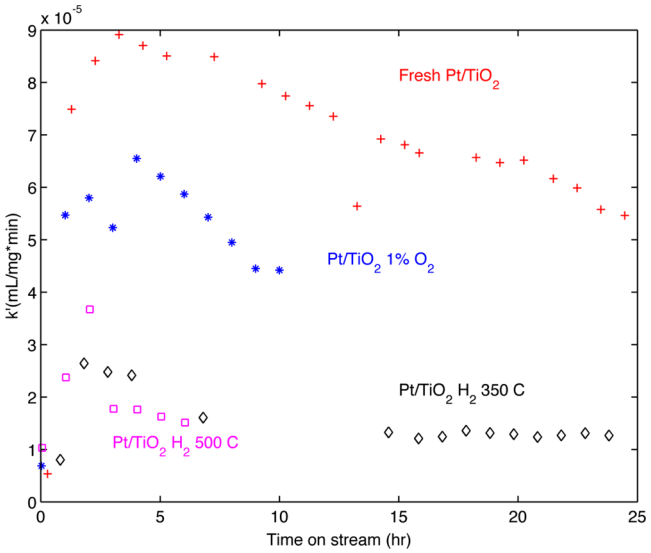

Figure 10. Rate constant for fresh and used Pt/TiO_2 catalyst after undergoing different treatments.

catalyst was then treated at 350 °C under flowing H_2 for 12 h to remove any C_3 poison molecules. Figure 9 shows that this treatment in 350 °C H_2 restored some decarboxylation activity, but the activity was still lower than that of the fresh catalyst. Next, we treated the Pt/TiO_2 catalyst in flowing H_2 at 500 °C for 12 h to remove poisons up to C_6. Again, the treatment restored activity with similar efficacy to the treatment at 350 °C. These results show that poisoning does play a role in deactivation, but the loss of activity due to poisoning is minor. Lastly, we performed controlled oxidation of the used catalyst at 500 °C for 12 h under 1% O_2 with the balance of N_2 to remove any carbon-containing species that were resistant to the H_2 treatments. Controlled oxidation restored the majority of the decarboxylation activity. Therefore, we suspect that coke formation is another cause of deactivation during hydrothermal decarboxylation of butyric acid over supported Pt catalysts. Deactivation by coking, which is reversible by controlled oxidation of the coke, typically exhibits deactivation orders of one or less.[28]

A final cause of deactivation in this system is collapse of the pore structure in the Pt/C catalyst. Pt/C in water alone at 350 °C produced 0.018 ± 0.002 μmol H_2 and 0.0062 ± 0.0019 μmol CO_2/mg Pt/C indicating that the support reacted with water under the experimental conditions. BET measurements of a used Pt/C catalyst and the fresh carbon support also show that the surface area of the used catalyst (220 m^2/g) was essentially the same as that of the fresh Vulcan XC-72 carbon (229 ± 6 m^2/g). The pore volume of the used catalyst, however, was 0.55 cm^3/g, whereas the original pore volume of the support is 1.42 ± 0.2 cm^3/g. The pore volume decreased during the reaction, and this decrease may have contributed to some of the lost activity.

CONCLUSIONS

The Pt/C catalyst experienced deactivation during decarboxylation of butyric acid in hot compressed water at 350 °C over the course of 24 h on stream. The deactivation of the catalyst is due to three separate phenomena. The carbon support, which typically is considered to be stable in hydrothermal environments, experienced loss of pore volume, indicative of pore collapse within the material. The Pt experienced deactivation through a combination of poisoning and coking. These modes were operative because of the tendency of Pt to dehydrogenate hydrocarbons. We believe that propylidene[23] or some other unsaturated C_3 molecular compound is responsible for catalyst poisoning. Thus, catalyst poisoning, coking, and structural degradation of the support all contributed to deactivation of the catalyst during hydrothermal decarboxylation of butyric acid.

The first-order deactivation rate constant for Pt/C at 350 °C was 0.063 ± 0.006 h^{-1}. As the catalyst deactivation occurred, however, the selectivity of the catalyst toward the desired decarboxylation product, propane, remained high. The research presented herein shows that Pt catalysts have potential for longevity in this application, but the hydrothermal conditions introduce complications not encountered in organic- or gas-phase decarboxylation processes. It is likely that adding a hydrogen source, whether internal or external, and/or modifying the catalyst to weaken the binding of unsaturated hydrocarbons could alleviate the issues of coking and catalyst poisoning. The irreversible catalyst deactivation noted here stemmed from degradation of the support, so identifying a more stable support can also contribute to a longer catalyst life.

AUTHOR INFORMATION

Corresponding Author

*E-mail: psavage@umich.edu.

Notes

The authors declare no competing financial interest.

ACKNOWLEDGMENTS

We gratefully acknowledge the National Science Foundation (Grant EFRI-0937992 and Award DMR-9871177), Rackham Graduate School at the University of Michigan, and Michigan College of Engineering for their financial support. We also thank Ryan Franck for experimental assistance.

ABBREVIATIONS

HDO, hydrodeoxygenation; GC, gas chromatography; TCD, thermal conductivity detector; FID, flame ionization detector; XRD, X-ray diffraction; ICP-OES, inductively coupled plasma−optical emission spectroscopy; TEM, transmission electron microscope; DRIFTS, diffuse reflectance infrared Fourier transform spectroscopy

REFERENCES

(1) Immer, J. G.; Kelly, M. J.; Lamb, H. H. Catalytic reaction pathways in liquid-phase deoxygenation of C18 free fatty acids. *Appl. Catal., A* **2010**, *375*, 134−139.

(2) Wang, W.-C.; Thapaliya, N.; Campos, A.; Stikeleather, L. F.; Roberts, W. L. Hydrocarbon fuels from vegetable oils via hydrolysis and thermo-catalytic decarboxylation. *Fuel* **2012**, *95*, 622−629.

(3) Kusdiana, D.; Saka, S. Effects of water on biodiesel fuel production by supercritical methanol treatment. *Bioresour. Technol.* **2004**, *91*, 289−295.

(4) Brown, T. M.; Duan, P.; Savage, P. E. Hydrothermal liquefaction and gasification of *Nannochloropsis* sp. *Energy Fuels* **2010**, *24*, 3639−3646.

(5) Barreiro, D. L.; Prins, W.; Ronsse, F.; Brilman, W. Hydrothermal liquefaction (HTL) of microalgae for biofuel production: State of the art review and future prospects. *Biomass Bioenergy* **2013**, *53*, 113−127 , 20th European Biomass Conference..

(6) Youssef, E. A.; Nakhla, G.; Charpentier, P. A. Oleic acid gasification over supported metal catalysts in supercritical water: Hydrogen production and product distribution. *Int. J. Hydrogen Energy* **2011**, *36*, 4830−4842.
(7) Yang, C.; Nie, R.; Fu, J.; Hou, Z.; Lu, X. Production of aviation fuel via catalytic hydrothermal decarboxylation of fatty acids in microalgae oil. *Bioresour. Technol.* **2013**, *146*, 569−573.
(8) Fu, J.; Lu, X.; Savage, P. E. Catalytic hydrothermal deoxygenation of palmitic acid. *Energy Environ. Sci.* **2010**, *3*, 311−317.
(9) Fu, J.; Lu, X.; Savage, P. E. Hydrothermal decarboxylation and hydrogenation of fatty acids over Pt/C. *ChemSusChem* **2011**, *4*, 481−486.
(10) Idesh, S.; Kudo, S.; Norinaga, K.; Hayashi, J. Catalytic hydrothermal reforming of jatropha oil in subcritical water for the production of green fuels: Characteristics of reactions over Pt and Ni catalysts. *Energy Fuels* **2013**, *27*, 4796−4803.
(11) Li, Y.; Somorjai, G. A. Nanoscale advances in catalysis and energy applications. *Nano Lett.* **2010**, *10*, 2289−2295.
(12) Mo, N.; Savage, P. E. Hydrothermal catalytic cracking of fatty acids with HZSM-5. *ACS Sustainable Chem. Eng.* **2014**, *2*, 88−94.
(13) Li, L.; Coppola, E.; Rine, J.; Miller, J. L.; Walker, D. Catalytic hydrothermal conversion of triglycerides to non-ester biofuels. *Energy Fuels* **2010**, *24*, 1305−1315.
(14) Mäki-Arvela, P.; Snåre, M.; Eränen, K.; Myllyoja, J.; Murzin, D. Continuous decarboxylation of lauric acid over Pd/C catalyst. *Fuel* **2008**, *87*, 3543−3549.
(15) Santillan-Jimenez, E.; Crocker, M. Catalytic deoxygenation of fatty acids and their derivatives to hydrocarbon fuels via decarboxylation/decarbonylation. *J. Chem. Technol. Biotechnol.* **2012**, *87*, 1041−1050.
(16) Immer, J. G.; Lamb, H. H. Fed-batch catalytic deoxygenation of free fatty acids. *Energy Fuels* **2010**, *24*, 5291−5299.
(17) Arend, M.; Nonnen, T.; Hoelderich, W. F.; Fischer, J.; Groos, J. Catalytic deoxygenation of oleic acid in continuous gas flow for the production of diesel-like hydrocarbons. *Appl. Catal., A* **2011**, *399*, 198−204.
(18) Elliott, D. C. Catalytic hydrothermal gasification of biomass. *Biofuels, Bioprod. Biorefin.* **2008**, *2*, 254−265.
(19) Ravenelle, R. M.; Diallo, F. Z.; Crittenden, J. C.; Sievers, C. Effects of Metal Precursors on the Stability and Observed Reactivity of Pt/γ − Al2O3 Catalysts in Aqueous Phase Reactions. *ChemCatChem.* **2012**, *4*, 492−494.
(20) Yuan, P.; Cheng, Z.; Jiang, W.; Zhang, R.; Yuan, W. Catalytic desulfurization of residual oil through partial oxidation in supercritical water. *J. Supercrit. Fluids* **2005**, *35*, 70−75.
(21) Snåre, M.; Kubicková, I.; Mäki-Arvela, P.; Eränen, K.; Murzin, D. Y. Heterogeneous catalytic deoxygenation of stearic acid for production of biodiesel. *Ind. Eng. Chem. Res.* **2006**, *45*, 5708−5715.
(22) Duan, P.; Savage, P. E. Upgrading of crude algal bio-oil in supercritical water. *Bioresour. Technol.* **2011**, *102*, 1899−1906.
(23) Lamb, H. H.; Sremaniak, L.; Whitten, J. L. Reaction pathways for butanoic acid decarboxylation on the (111) surface of a Pd nanoparticle. *Surf. Sci.* **2013**, *607*, 130−137.
(24) Ho, V. T. T.; Pillai, K. C.; Chou, H.-L.; Pan, C.-J.; Rick, J.; Su, W.-N.; Hwang, B.-J.; Lee, J.-F.; Sheu, H.-S.; Chuang, W.-T. Robust non-carbon $Ti_{0.7}Ru_{0.3}O_2$ support with co-catalytic functionality for Pt: Enhances catalytic activity and durability for fuel cells. *Energy Environ. Sci.* **2011**, *4*, 4194−4200.
(25) Matsumura, Y.; Xu, X.; Antal, J. M. Gasification characteristics of an activated carbon in supercritical water. *Carbon* **1997**, *35*, 819−824.
(26) Fu, J.; Shi, F.; Thompson, L. T.; Lu, X.; Savage, P. E. Activated carbons for hydrothermal decarboxylation of fatty acids. *ACS Catal.* **2011**, *1*, 227−231.
(27) Luo, N.; Fu, X.; Cao, F.; Xiao, T.; Edwards, P. P. Glycerol aqueous phase reforming for hydrogen generation over Pt catalyst - Effect of catalyst composition and reaction conditions. *Fuel* **2008**, *87*, 3483−3489.
(28) Hughes, R. *Deactivation of Catalysts*; Academic Press: London, 1984; p 265.